Modeling Missing Data in Clinical Time Series with RNNs

Zachary C. Lipton ZLIPTON@CS.UCSD.EDU
Department of Computer Science and Engineering
University of California, San Diego
La Jolla, CA 92093, USA

David C. Kale KALE@ISI.EDU
USC Information Sciences Institute
Marina del Rey, CA, USA

Randall Wetzel RWETZEL@CHLA.USC.EDU
Laura P. and Leland K. Whittier Virtual Pediatric Intensive Care Unit
Children's Hospital LA
Los Angeles, CA 90089

Abstract

We demonstrate a simple strategy to cope with missing data in sequential inputs, addressing the task of multilabel classification of diagnoses given clinical time series. Collected from the pediatric intensive care unit (PICU) at Children's Hospital Los Angeles, our data consists of multivariate time series of observations. The measurements are irregularly spaced, leading to missingness patterns in temporally discretized sequences. While these artifacts are typically handled by imputation, we achieve superior predictive performance by treating the artifacts as features. Unlike linear models, recurrent neural networks can realize this improvement using only simple binary indicators of missingness. For linear models, we show an alternative strategy to capture this signal. Training models on missingness patterns only, we show that for some diseases, *what tests are run* can as predictive as the results themselves.

1. Introduction

For each admitted patient, hospital intensive care units record large amounts data in electronic health records (EHRs). Clinical staff routinely chart vital signs during hourly rounds and when patients are unstable. EHRs record lab test results and medications as they are ordered or delivered by physicians and nurses. As a result, EHRs contain rich sequences of clinical observations depicting both patients' health and care received. We would like to mine these time series to build accurate predictive models for diagnosis and other applications. Recurrent neural networks (RNNs) are well-suited to learning sequential or temporal relationships from such time series. RNNs offer unprecedented predictive power in myriad sequence learning domains, including natural language processing, speech, video, and handwriting. Recently, Lipton et al. (2016) demonstrated the efficacy of RNNS for multilabel classification of diagnoses in clinical time series data.

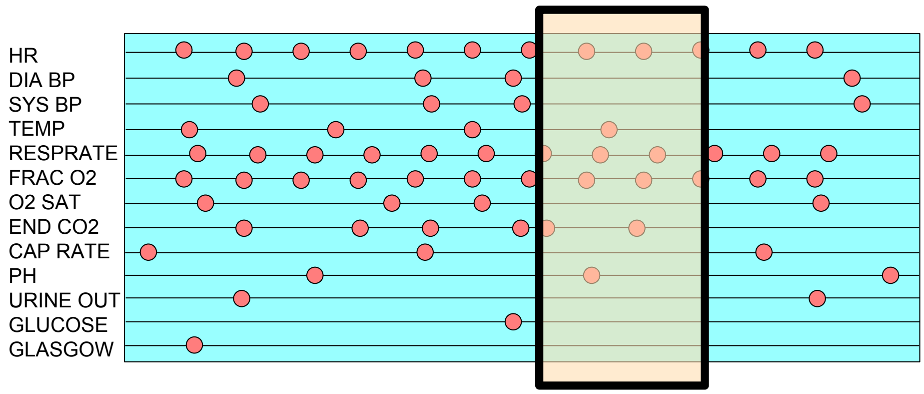

Figure 1: Missingness artifacts created by discretization

However, medical time series data present modeling problems not found in the clean academic datasets on which most RNN research focuses. Clinical observations are recorded irregularly, with measurement frequency varying between patients, across variables, and even over time. In one common modeling strategy, we represent these observations as a sequence with discrete, fixed-width time steps. Problematically, the resulting sequences often contain missing values (Marlin et al., 2012). These values are typically not missing at random, but reflect decisions by caregivers. Thus, the pattern of recorded measurements contain potential information about the state of the patient. However, most often, researchers fill missing values using heuristic or unsupervised imputation (Lasko et al., 2013), ignoring the potential predictive value of the missingness itself.

In this work we extend the methodology of Lipton et al. (2016) for RNN-based multilabel prediction of diagnoses. We focus on data gathered from the Children's Hospital Los Angeles pediatric intensive care unit (PICU). Unlike Lipton et al. (2016), who approach missing data via heuristic imputation, we directly model missingness as a feature, achieving superior predictive performance. Unlike linear models, RNNs can realize this improvement using only simple binary indicators for missingness. However, while RNNs can learn arbitrary functions of the missingness indicators and previous inputs, linear models can only learn substitution values. For linear models, we introduce an alternative strategy to capture this signal using a small number of simple hand-engineered features. Additionally, we evaluate RNNs, multilayer perceptrons (MLPs), and linear models trained on missingness patterns only, showing that for several diseases, *what tests are run* can be as predictive as the actual measurements. While we focus on classifying diagnoses, our methods can be applied to any predictive modeling problem involving sequence data and missing values, such as early prediction of sepsis (Henry et al., 2015) or real-time risk modeling (Wiens et al., 2012).

It is worth noting that we may not want our predictive models to rely upon the patterns of treatment, as argued by Caruana et al. (2015). Once deployed, our models may influence the treatment protocols, shifting the distribution of future data, and thus invalidating their predictions. Nonetheless, doctors at present often utilize knowledge of past care, and treatment signal can leak into the actual measurements themselves in a way that is detectable by sufficiently powerful models. As a final contribution of this paper, we present a critical discussion of these practical and philosophical issues.

2. Data

Our dataset consists of patient records extracted from the EHR system at CHLA (Marlin et al., 2012; Che et al., 2015) as part of an IRB-approved study. In all, the dataset contains $10,401$ PICU episodes. Each episode describes the stay of one patient in the PICU for a period of at least 12 hours. In addition, each patient record contains a static set of diagnostic codes, annotated by physicians either during or after each PICU visit.

2.1 Inputs

In their rawest representation, episodes consist of irregularly spaced measurements of 13 variables: diastolic and systolic blood pressure, peripheral capillary refill rate, end-tidal CO_2 ($ETCO_2$), fraction of inspired O_2 (FIO_2), total Glascow coma scale, blood glucose, heart rate, pH, respiratory rate, blood oxygen saturation, body temperature, and urine output. To render our data suitable for learning with RNNs, we convert to discrete sequences of hourly time steps, where time step t covers the interval between hours t and $t+1$, closed on the left but open on the right. Because actual admission times are not recorded reliably, we use the time of the first recorded observation as time step $t = 0$. We combine multiple measurements of the same variable within the same hour window by taking their mean.

Vital signs, such as heart rate, are typically measured about once per hour, while lab tests requiring a blood draw (e.g., glucose) are measured on the order of once per day (see appendix B for measurement frequency statistics). In addition, the timing of and time between observations varies across patients and over time. The resulting sequential representation have many missing values, and some variables missing altogether.

Note that our methods can be sensitive to the duration of our discrete time step. For example, halving the duration would double the length of the sequences, making learning by backpropagation through time more challenging (Bengio et al., 1994). For our data, such cost would not be justified because the most frequently measured variables (vital signs) are only recorded about once per hour. For higher frequency recordings of variables with faster dynamics, a shorter time step might be warranted.

To better condition our inputs, we scale each variable to the $[0, 1]$ interval, using expert-defined ranges. Additionally, we correct for differences in heart rate, respiratory rate, (Fleming et al., 2011) and blood pressure (NHBPEP Working Group 2004) due to age and gender using tables of normal values from large population studies.

2.2 Diagnostic labels

In this work, we formulate *phenotyping* (Oellrich et al, 2015) as multilabel classification of sequences. Our labels include 429 distinct diagnosis codes from an in-house taxonomy at CHLA, similar to ICD-9 codes (World Health Organization, 2004) commonly used in medical informatics research. These labels include a wide range of acute conditions, such as acute respiratory distress, congestive heart failure, and sepsis. A full list is given in appendix A. We focus on the 128 most frequent, each having at least 50 positive examples in our dataset.

Naturally, the diagnoses are not mutually exclusive. In our data set, the average patient is associated with 2.24 diagnoses. Additionally, the base rates of the diagnoses vary widely (see appendix A).

3. Recurrent Neural Networks for Multilabel Classification

While our focus in this paper is on missing data, for completeness, we review the LSTM RNN architecture for performing multilabel classification of diagnoses introduced by Lipton et al. (2016). Formally, given a series of observations $\boldsymbol{x}^{(1)}, ..., \boldsymbol{x}^{(T)}$, we desire a classifier to generate hypotheses $\hat{\boldsymbol{y}}$ of the true labels $\boldsymbol{y}$, where each input $\boldsymbol{x}^t \in \mathbb{R}^D$ and the output $\hat{\boldsymbol{y}} \in [0, 1]^K$. Here, D denotes the input dimension, K denotes the number of labels, t indexes sequence steps, and for any example, T denotes the length of that sequence.

Our proposed RNN uses LSTM memory cells (Hochreiter and Schmidhuber, 1997) with forget gates (Gers et al., 2000) but without peephole connections (Gers et al., 2003). As output, we use a fully connected layer followed by an element-wise logistic activation function σ. We apply *log loss* (binary cross-entropy) as the loss function at each output node.

The following equations give the update for a layer of memory cells $\boldsymbol{h}_l^{(t)}$, where $\boldsymbol{h}_{l-1}^{(t)}$ stands for the previous layer at the same sequence step (a previous LSTM layer or the input $\boldsymbol{x}^{(t)}$) and $\boldsymbol{h}_l^{(t-1)}$ stands for the same layer at the previous sequence step:

$$
\begin{aligned}
\boldsymbol{g}_l^{(t)} &= \phi(W_l^{\mathrm{gx}} \boldsymbol{h}_{l-1}^{(t)} + W_l^{\mathrm{gh}} \boldsymbol{h}_l^{(t-1)} + \boldsymbol{b}_l^{\mathrm{g}}) \\
\boldsymbol{i}_l^{(t)} &= \sigma(W_l^{\mathrm{ix}} \boldsymbol{h}_{l-1}^{(t)} + W_l^{\mathrm{ih}} \boldsymbol{h}_l^{(t-1)} + \boldsymbol{b}_l^{\mathrm{i}}) \\
\boldsymbol{f}_l^{(t)} &= \sigma(W_l^{\mathrm{fx}} \boldsymbol{h}_{l-1}^{(t)} + W_l^{\mathrm{fh}} \boldsymbol{h}_l^{(t-1)} + \boldsymbol{b}_l^{\mathrm{f}}) \\
\boldsymbol{o}_l^{(t)} &= \sigma(W_l^{\mathrm{ox}} \boldsymbol{h}_{l-1}^{(t)} + W_l^{\mathrm{oh}} \boldsymbol{h}_l^{(t-1)} + \boldsymbol{b}_l^{\mathrm{o}}) \\
\boldsymbol{s}_l^{(t)} &= \boldsymbol{g}_l^{(t)} \odot \boldsymbol{i}_l^{(i)} + \boldsymbol{s}_l^{(t-1)} \odot \boldsymbol{f}_l^{(t)} \\
\boldsymbol{h}_l^{(t)} &= \phi(\boldsymbol{s}_l^{(t)}) \odot \boldsymbol{o}_l^{(t)}
\end{aligned}
$$

In these equations, σ stands for an element-wise application of the *logistic* function, ϕ stands for an element-wise application of the *tanh* function, and $\odot$ is the Hadamard (element-wise) product. The input, output, and forget gates are denoted by $\boldsymbol{i}$, $\boldsymbol{o}$, and $\boldsymbol{f}$ respectively, while $\boldsymbol{g}$ is the input node and has a *tanh* activation.

The loss at a single sequence step is the average *log loss* calculated across all labels:

$$
\mathrm{loss}(\hat{\boldsymbol{y}}, \boldsymbol{y}) = \frac{1}{K} \sum_{l=1}^{l=K} -(y_l \cdot \log(\hat{y}_l) + (1 - y_l) \cdot \log(1 - \hat{y}_l)).
$$

To overcome the difficulty of learning to pass information across long sequences, we use the *target replication* strategy proposed by Lipton et al. (2016), in which we replicate the static targets at each sequence step providing a local error signal. This technique is also motivated by our problem: we desire to make accurate predictions even if the sequence were truncated (as in early-warning systems). To calculate loss, we take a convex combination of the final step loss and the average of the losses over predictions $\hat{\boldsymbol{y}}^{(t)}$ at all steps t:

$$\alpha \cdot \frac{1}{T} \sum_{t=1}^{T} \text{loss}(\hat{\boldsymbol{y}}^{(t)}, \boldsymbol{y}^{(t)}) + (1 - \alpha) \cdot \text{loss}(\hat{\boldsymbol{y}}^{(T)}, \boldsymbol{y}^{(T)})$$

where $\alpha \in [0, 1]$ is a hyper-parameter determining the relative importance of performance on the intermediary vs. final targets. At inference time, we consider only the output at the final step.

4. Missing Data

In this section, we explain our procedures for imputation, missing data indicator sequences, engineering features of missing data patterns.

4.1 Imputation

To address the missing data problem, we consider two different imputation strategies (forward-filling and zero imputation), as well as direct modeling via indicator variables. Because imputation and direct modeling are not mutually exclusive, we also evaluate them in combination. Suppose that $x_i^{(t)}$ is "missing." In our *zero-imputation* strategy, we simply set $x_i^{(t)} := 0$ whenever it is missing. In our *forward-filling* strategy, we impute $x_i^{(t)}$ as follows:

- If there is at least one previously recorded measurement of variable i at a time $t' < t$, we perform forward-filling by setting $x_i^{(t)} := x_i^{(t')}$.
- If there is no previous recorded measurement (or if the variable is missing entirely), then we impute the median estimated over all measurements in the training data.

This strategy is motivated by the intuition that clinical staff record measurements at intervals proportional to rate at which they are believed or observed to change. Heart rate, which can change rapidly, is monitored much more frequently than blood pH. Thus it seems reasonable to assume that a value has changed little since the last time it was measured.

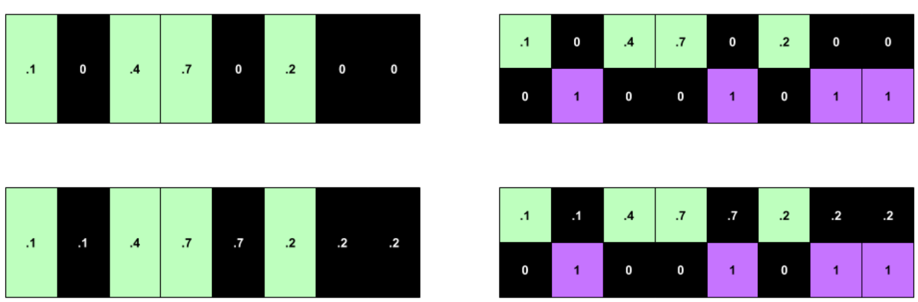

Figure 2: (top left) no imputation or indicators, (bottom left) imputation absent indicators, (top right) indicators but no imputation, (bottom right) indicators and imputation. Time flows from left to right.

4.2 Learning with Missing Data Indicators

Our *indicator variable* approach to missing data consists of augmenting our inputs with binary variables $m_i^{(t)}$ for every $x_i^{(t)}$, where $m_i^{(t)} := 1$ if $x_i^{(t)}$ is imputed and 0 otherwise. Through their hidden state computations, RNNs can use these indicators to learn arbitrary functions of the past observations and missingness patterns. However, given the same data, linear models can only learn hard substitution rules. To see why, consider a linear model that outputs prediction $f(z)$, where $z = \sum_i w_i \cdot x_i$. With indicator variables, we might say that $z = \sum_i w_i \cdot x_i + \sum_i \theta_i \cdot m_i$ where θ_i are the weights for each m_i. If x_i is set to 0 and m_i to 1, whenever the feature x_i is missing, then the impact on the output $\theta_i \cdot m_i = \theta_i$ is exactly equal to the contribution $w_i \cdot x_i^*$ for some $x_i^* = \theta_i / w_i$. In other words, the linear model can only use the indicator in a way that depends neither on the previously observed values $(x_i^1 ... x_i^{t-1})$, nor any other evidence in the inputs.

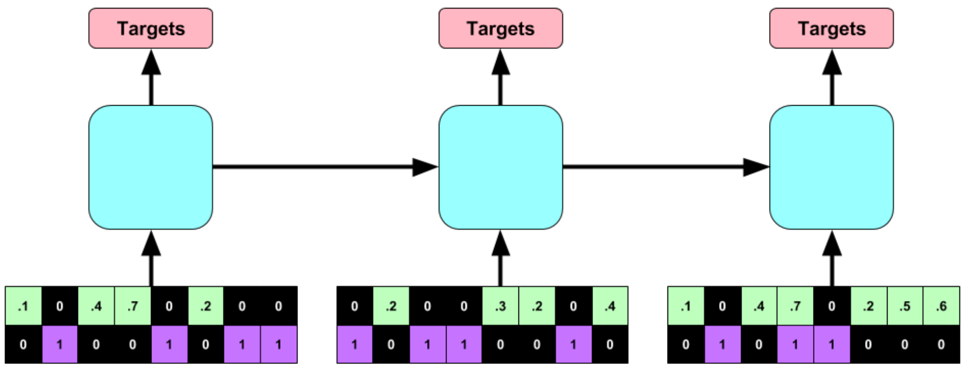

Figure 3: Depiction of RNN zero-filled inputs and missing data indicators.

Note that for a linear model, the impact of a missing data indicator on predictions must be monotonic. In contrast, the RNN might infer that for one patient heart rate is missing because they went for a walk, while for another it might signify an emergency. Also note that even without indicators, the RNN might learn to recognize *filled-in* vs *real* values. For example, with forward-filling, the RNN could learn to recognize exact repeats. For zero-filling, the RNN could recognize that values set to exactly 0 were likely missing measurements.

4.3 Hand-engineered missing data features

To overcome the limits of the linear model, we also designed features from the indicator sequences. As much as possible, we limited ourselves to features that are simple to calculate, intuitive, and task-agnostic. The first is a binary indicator for whether a variable was measured *at all*. Additionally, we compute the mean and standard deviation of the indicator sequence. The mean captures the frequency with which each variable is measured which carries information about the severity of a patient's condition. The standard deviation, on the other hand, computes a non-monotonic function of frequency that is maximized when a variable is missing exactly 50% of the time. We also compute the frequency with which a variable switches from measured to missing or vice versa across adjacent sequence steps.

Finally, we add features that capture the relative timing of the first and last measurements of a variable, computed as the number of hours until the measurement divided by the length of the full sequence.

5. Experiments

We now present the training details and empirical findings of our experiments. Our LSTM RNNs each have 2 hidden layers of 128 LSTM cells each, non-recurrent dropout of 0.5, and ℓ_2^2 weight decay of 10^{-6}. We train on 80% of data, setting aside 10% each for validation and testing. We train each RNN for 100 epochs, retaining the parameters corresponding to the epoch with the lowest validation loss.

We compare the performance of RNNs against logistic regression and multilayer perceptrons (MLPs). We apply ℓ_2 regularization to the logistic regression model. The MLP has 3 hidden layers with 500 nodes each, rectified linear unit activations, and dropout (with probability of 0.5), choosing the number of layers and nodes by validation performance. We train the MLP using stochastic gradient descent with momentum.

We evaluate each baseline with two sets of features: raw and hand-engineered. Note that our baselines cannot be applied directly to variable-length inputs. For the raw features, we concatenate three 12-hour subsequences, one each from the beginning, middle, and end of the time series. For shorter time series, these intervals may overlap. Thus raw representations contain $2 \times 3 \times 12 \times 13 = 936$ features. We train each baseline on five different combinations of raw inputs: (1) measurements with zero-filling, (2) measurements with forward-filling, (2) measurements with zero-filling + missing data indicators, (4) forward-filling + missing data indicators, and (5) missing data indicators only.

Our hand-engineered features capture central tendencies, variability, extremes, and trends. These include the first and last measurements and their difference, maximum and minimum values, mean and standard deviation, median and 25th and 75th percentiles, and the slope and intercept of least squares line fit. We also computed the 8 missing data features described in section 4. We improve upon the baselines in Lipton et al. (2016) by computing the hand-engineered features over different windows of time, giving them access to greater temporal information and enabling them to better model patterns of missingness. We extract hand-engineered features from the entire time series and from three possibly overlapping intervals: the first and last 12 hours and the interval between (for shorter sequences, we instead use the middle 12 hours). This yields a total of $4 \times 12 \times 13 = 624$ and $4 \times 8 \times 13 = 416$ hand-engineered measurement and missing data features, respectively. We train baseline models on three different combinations of hand-engineered features: (1) measurement-only, (2) indicator-only, and (3) measurement and indicator.

We evaluate all models on the same training, validation, and test splits. Our evaluation metrics include area under the ROC curve (AUC) and F1 score (with threshold chosen based on validation performance). We report both micro-averaged (calculated across all predictions) and macro-averaged (calculated separately on each label, then averaged) measures to mitigate the weaknesses in each (Lipton et al., 2014). Finally we also report precision at 10, whose maximum is 0.2238 because we have on average 2.238 diagnoses per patient. This metric seems appropriate because we could imagine this technology would be integrated into a diagnostic assistant. In that case, its role might be to suggest the most likely diagnoses among which a professional doctor would choose. Precision at 10 evaluates the quality of the top 10 suggestions.

Classification performance for 128 ICU phenotypes

Model	Micro AUC	Macro AUC	Micro F1	Macro F1	P@10
Base Rate	0.7128	0.5	0.1346	0.0343	0.0788
Best Possible	1.0	1.0	1.0	1.0	0.2281
Logistic Regression					
Log Reg - Zeros	0.8108	0.7244	0.2149	0.0999	0.1014
Log Reg - Impute	0.8201	0.7455	0.2404	0.1189	0.1038
Log Reg - Zeros & Indicators	0.8143	0.7269	0.2239	0.1082	0.1017
Log Reg - Impute & Indicators	0.8242	0.7442	0.2467	0.1234	0.1045
Log Reg - Indicators Only	0.7929	0.6924	0.1952	0.0889	0.0939
Multilayer Perceptron					
MLP - Zeros	0.8263	0.7502	0.2344	0.1072	0.1048
MLP - Impute	0.8376	0.7708	0.2557	0.1245	0.1031
MLP - Zeros & Indicators	0.8381	0.7705	0.2530	0.1224	0.1067
MLP - Impute & Indicators	0.8419	0.7805	0.2637	0.1296	0.1082
MLP - Indicators Only	0.8112	0.7321	0.1962	0.0949	0.0947
LSTMs					
LSTM - Zeros	0.8662	0.8133	0.2909	0.1557	0.1176
LSTM - Impute	0.8600	0.8062	0.2967	0.1569	0.1159
LSTM - Zeros & Indicators	**0.8730**	**0.8250**	**0.3041**	**0.1656**	**0.1215**
LSTM - Impute & Indicators	0.8689	0.8206	0.3027	0.1609	0.1196
LSTM - Indicators Only	0.8409	0.7834	0.2403	0.1291	0.1074
Models using Hand-Engineered Features					
Log Reg HE	0.8396	0.7714	0.2708	0.1327	0.1118
Log Reg HE Indicators	0.8472	0.7752	0.2841	0.1376	0.1165
Log Reg HE Indicators Only	0.8187	0.7322	0.2287	0.1001	0.1020
MLP HE	0.8599	0.8052	0.2953	0.1556	0.1168
MLP HE Indicators	0.8669	0.8160	0.2954	0.1610	0.1202
MLP HE Indicators Only	0.8371	0.7682	0.2351	0.1179	0.1028

Table 1: Performance on aggregate metrics for logistic regression (Log Reg), MLP, and LSTM classifiers with and without imputation and missing data indicators.

5.1 Results

The best overall model by all metrics (micro AUC of 0.8730) is an LSTM with zero-imputation and missing data indicators. It outperforms both the strongest MLP baseline and LSTMs absent missing data indicators. For the LSTMs using either imputation strategy, adding the missing data indicators improves performance in all metrics. While all models improve with access to missing data indicators, this information confers less benefit to the raw input linear baselines, consistent with theory discussed in subsection 4.2.

The results achieved by logistic regression with hand-engineered features indicates that our simple hand-engineered missing data features do a reasonably good job of capturing important information that neural networks are able to mine automatically. We also find that LSTMs (with or without indicators) appear to perform better with zero-filling than with with imputed values. Interestingly, this is not true for either baseline. It suggests that the LSTM may be learning to recognize missing values implicitly by recognizing a tight range about the value zero and inferring that this is a missing value. If this is true, perhaps imputation interferes with the LSTM's ability to implicitly recognize missing values. Overall, the ability to implicitly infer missingness may have broader implications. It suggests that we might never completely hide this information from a sufficiently powerful model.

6. Related Work

This work builds upon research relating to missing values and machine learning for medical informatics. The basic RNN methodology for phenotyping derives from Lipton et al. (2016), addressing a dataset and problem described by Che et al. (2015). The methods rely upon LSTM RNNs (Hochreiter and Schmidhuber, 1997; Gers et al., 2000) trained by backpropagation through time (Hinton et al., 2006; Werbos, 1988). A comprehensive perspective on the history and modern applications of RNNs is provided by Lipton et al. (2015), while Lipton et al. (2016) list many of the previous works that have applied neural networks to digital health data.

While a long and rich literature addresses pattern recognition with missing data (Cohen and Cohen, 1975; Allison, 2001), most of this literature addresses fixed-length feature vectors (García-Laencina et al., 2010; Pigott, 2001). Indicator variables for missing data were first proposed by Cohen and Cohen (1975), but we could not find papers that combine missing data indicators with RNNs. Only a handful of papers address missing data in the context of RNNS. Bengio and Gingras (1996) demonstrate a scheme by which the RNN learns to fill in the missing values such that the filled-in values minimize output error. In 2001, Parveen and Green (2001) built upon this method to improve automatic speech recognition. Barker et al. (2001) suggests using a mask of indicators in a scheme for weighting the contribution of reliable vs corrupted data in the final prediction. Tresp and Briegel (1998) address missing values by combining an RNN with a linear state space model to handle uncertainty. This paper may be one of the first to engineer explicit features of missingness patterns in order to improve discriminative performance. Also, to our knowledge, we are the first to harness patterns of missing data to improve the classification of critical care phenotypes.

7. Discussion

Data processing and discriminative learning have often been regarded as separate disciplines. Through this separation of concerns, the complementarity of missing data indicators and training RNNs for classification has been overlooked. This paper proposes that patterns of missing values are an underutilized source of predictive power and that RNNs, unlike linear models, can effectively mine this signal from sequences of indicator values. Our hypotheses are confirmed by empirical evidence. Additionally, we introduce and confirm the utility of a simple set of features, engineered from the sequence of missingness indicators, that can improve performance of linear models. These techniques are simple to implement and broadly applicable and seem likely to confer similar benefits on other sequential prediction tasks, when data is missing not at random. One example might include financial data, where failures to report accounting details could suggest internal problems at a company.

7.1 The Perils and Inevitability of Modeling Treatment Patterns

For medical applications, the predictive power of missing data raises important philosophical concerns. We train models with supervised learning, and verify their utility by assessing the accuracy of their classifications on hold-out test data. However, in practice, we hope to make treatment decisions based on these predictions, exposing a fundamental incongruity between the problem on which our models are trained and those for which they are ultimately deployed. As articulated in Lipton (2016), these supervised models, trained offline, cannot account for changes that their deployment might confer upon the real world, possibly invalidating their predictions. Caruana et al. (2015) present a compelling case in which a pneumonia risk model predicted a lower risk of death for patients who also have asthma. The better outcomes of the asthma patients, as it turns out, owed to the more aggressive treatment they received. The model, if deployed, might be used to choose less aggressive treatment for the patients with both pneumonia and asthma, clearly a sub-optimal course of action.

On the other hand, to some degree, learning from treatment signal may be inevitable. Any imputation might leak some information about which values are likely imputed and which are not. Thus any sufficiently powerful supervised model might catch on to some amount of missingness signal, as was the case in our experiments with the LSTM using zero-filled missing values. Even physiologic measurements contain information owing to patterns of treatment, possibly reflecting the medications patients receive and the procedures they undergo.

Sometimes the patterns of treatments may be a reasonable and valuable source of information. Doctors already rely on this kind of signal habitually: they read through charts, noting which other doctors have seen a patient, inferring what their opinions might have been from which tests they ordered. While, in some circumstances, it may be problematic for learning models to rely on this signal, removing it entirely may be both difficult and undesirable.

7.2 Complex Models or Complex Features?

Our work also shows that using only simple features, RNNs can achieve state of the art performance classifying clinical time series. The RNNs far outperform linear models. Still, in our experience, there is a strong bias among practitioners toward more familiar models even when they require substantial feature engineering.

In our experiments, we undertook extensive efforts to engineer features to boost the performance of both linear models and MLPs. Ultimately, while RNNs performed best on raw data, we could approach its performance with an MLP and significantly improve the linear model by using hand-engineered features and windowing. A question then emerges: how should we evaluate the trade-off between more complex models and more complex features? To the extent that linear models are believed to be more interpretable than neural networks, most popular notions of interpretability hinge upon the intelligibility of the features (Lipton, 2016). When performance of the linear model comes at the price of this intelligibility, we might ask if this trade-off undermines the linear model's chief advantage. Additionally, such a model, while still inferior to the RNN, relies on application-specific features less likely to be useful on other datasets and tasks. In contrast, RNNs seem better equipped to generalize to different tasks. While the model may be complex, the inputs remain intelligible, opening the possibility to various post-hoc interpretations (Lipton, 2016).

7.3 Future Work

We see several promising next steps following this work. First, we would like to validate this methodology on tasks with more immediate clinical impact, such as predicting sepsis, mortality, or length of stay. Second, we'd like to extend this work towards predicting clinical decisions. Called policy imitation in the reinforcement literature, such work could pave the way to providing real-time decision support. Finally, we see machine learning as cooperating with a human decision-maker. Thus a machine learning model needn't always make a prediction/classification; it could also abstain. We hope to make use of the latest advances in mining uncertainty information from neural networks to make confidence-rated predictions.

8. Acknowledgments

Zachary C. Lipton was supported by the Division of Biomedical Informatics at the University of California, San Diego, via training grant (T15LM011271) from the NIH/NLM. David Kale was supported by the Alfred E. Mann Innovation in Engineering Doctoral Fellowship. The VPICU was supported by grants from the Laura P. and Leland K. Whittier Foundation. We acknowledge NVIDIA Corporation for Tesla K40 GPU hardware donation and Professors Charles Elkan and Greg Ver Steeg for their support and advice.

References

Paul D Allison. *Missing data*. 2001.

Jon Barker, Phil Green, and Martin Cooke. Linking auditory scene analysis and robust asr by missing data techniques. 2001.

Yoshua Bengio and Francois Gingras. Recurrent neural networks for missing or asynchronous data. 1996.

Yoshua Bengio, Patrice Simard, and Paolo Frasconi. Learning long-term dependencies with gradient descent is difficult. *Neural Networks, IEEE Transactions on*, 1994.

Rich Caruana, Yin Lou, Johannes Gehrke, Paul Koch, Marc Sturm, and Noemie Elhadad. Intelligible models for healthcare: Predicting pneumonia risk and hospital 30-day readmission. In *KDD*, 2015.

Zhengping Che, David C. Kale, Wenzhe Li, Mohammad Taha Bahadori, and Yan Liu. Deep computational phenotyping. In *KDD*. ACM, 2015.

Jacob Cohen and Patricia Cohen. Applied multiple regression/correlation analysis for the behavioral sciences. 1975.

Susannah Fleming, Matthew Thompson, Richard Stevens, Carl Heneghan, Annette Plüddemann, Ian Maconochie, Lionel Tarassenko, and David Mant. Normal ranges of heart rate and respiratory rate in children from birth to 18 years: A systematic review of observational studies. *The Lancet*, 2011.

Pedro J García-Laencina, José-Luis Sancho-Gómez, and Aníbal R Figueiras-Vidal. Pattern classification with missing data: a review. *Neural Computing and Applications*, 2010.

Felix A. Gers, Jürgen Schmidhuber, and Fred Cummins. Learning to forget: Continual prediction with LSTM. *Neural Computation*, 2000.

Felix A. Gers, Nicol N. Schraudolph, and Jürgen Schmidhuber. Learning precise timing with LSTM recurrent networks. *JMLR*, 2003.

Katharine E Henry, David N Hager, Peter J Pronovost, and Suchi Saria. A targeted real-time early warning score (trewscore) for septic shock. *Science Translational Medicine*, 2015.

Geoffrey E. Hinton, Simon Osindero, and Yee Whye Teh. A fast learning algorithm for deep belief nets. *Neural Computation*, 2006.

Sepp Hochreiter and Jürgen Schmidhuber. Long short-term memory. *Neural Computation*, 1997.

Thomas A. Lasko, Joshua C. Denny, and Mia A. Levy. Computational phenotype discovery using unsupervised feature learning over noisy, sparse, and irregular clinical data. *PLoS ONE*, 2013.

Zachary C Lipton. The mythos of model interpretability. *ICML Workshop on Human Interpretability in Machine Learning*, 2016.

Zachary C Lipton, Charles Elkan, and Balakrishnan Naryanaswamy. Optimal thresholding of classifiers to maximize F1 measure. In *Machine Learning and Knowledge Discovery in Databases*. 2014.

Zachary C. Lipton, John Berkowitz, and Charles Elkan. A critical review of recurrent neural networks for sequence learning. *arXiv:1506.00019*, 2015.

Zachary C Lipton, David C Kale, Charles Elkan, and Randall Wetzell. Learning to diagnose with lstm recurrent neural networks. *ICLR*, 2016.

Ben M. Marlin, David C. Kale, Robinder G. Khemani, and Randall C. Wetzel. Unsupervised pattern discovery in electronic health care data using probabilistic clustering models. In *Proceedings of the 2nd ACM SIGHIT International Health Informatics Symposium*, 2012.

National High Blood Pressure Education Program Working Group on Children and Adolescents. The fourth report on the diagnosis, evaluation, and treatment of high blood pressure in children and adolescents. *Pediatrics*, 2004.

Anika Oellrich et al. The digital revolution in phenotyping. *Briefings in Bioinformatics*, 2015.

Shahla Parveen and P Green. Speech recognition with missing data using recurrent neural nets. In *NIPS*, 2001.

Therese D Pigott. A review of methods for missing data. *Educational research and evaluation*, 2001.

Volker Tresp and Thomas Briegel. A solution for missing data in recurrent neural networks with an application to blood glucose prediction. In *NIPS*. 1998.

Paul J Werbos. Generalization of backpropagation with application to a recurrent gas market model. *Neural Networks*, 1988.

Jenna Wiens, Eric Horvitz, and John V Guttag. Patient risk stratification for hospital-associated c. diff as a time-series classification task. In *NIPS*, 2012.

World Health Organization. *International statistical classification of diseases and related health problems*. World Health Organization, 2004.

Appendix A. Per Diagnosis Classification Performance

In this appendix, we provide per-diagnosis AUC and F1 scores for three representative LSTM models trained with imputed measurements, with imputation plus missing indicators, and with indicators only. By comparing performance on individual diagnoses, we can gain some insight into the relationship between missing values and different conditions. Rows are sorted in descending order based on the F1 score of the imputation plus indicators model. It is worth noting that F1 scores are sensitive to threshold, which we chose in order to optimize per-disease validation F1, sometimes based on a very small number of positive cases. Thus, there are cases where one model will have superior AUC but worse F1.

Classifier Performance on Each Diagnostic Code, Sorted by F1

		Msmt.		**Msmt. + indic.**		**Indic.**	
Condition	Base rate	AUC	F1	AUC	**F1**	AUC	F1
Diabetes mellitus with ketoacidosis	0.0125	1.0000	0.8889	0.9999	**0.9333**	0.9906	0.7059
Asthma with status asthmaticus	0.0202	0.9384	**0.6800**	0.8907	0.6383	0.8652	0.5417
Scoliosis (idiopathic)	0.1419	0.9143	**0.6566**	0.8970	0.6174	0.8435	0.5235
Tumor, cerebral	0.0917	0.8827	**0.5636**	0.8799	0.5560	0.8312	0.4627
Renal transplant, status post	0.0122	0.9667	0.2963	0.9544	0.4762	0.9490	**0.5600**
Liver transplant, status post	0.0106	0.7534	0.3158	0.8283	**0.4762**	0.8271	0.2581
Acute respiratory distress syndrome	0.0193	0.9696	0.3590	0.9705	**0.4557**	0.9361	0.3333
Developmental delay	0.0876	0.8108	**0.4382**	0.8382	0.4331	0.6912	0.2366
Diabetes insipidus	0.0127	0.9220	0.2727	0.9486	**0.4286**	0.9266	0.4000
End stage renal disease (on dialysis)	0.0241	0.8548	0.2778	0.8800	0.4186	0.9043	**0.4255**
Seizure disorder	0.0816	0.7610	0.3694	0.7937	**0.4059**	0.6431	0.1957
Acute respiratory failure	0.0981	0.8414	0.4128	0.8391	0.3835	0.8358	**0.4542**
Cystic fibrosis	0.0076	0.8628	0.2353	0.8740	**0.3810**	0.8189	0.0000
Septic shock	0.0316	0.8296	0.3363	0.8911	**0.3750**	0.8506	0.1429
Respiratory distress, other	0.0716	0.8411	**0.3873**	0.8502	0.3719	0.7857	0.2143
Intracranial injury, closed	0.0525	0.8886	0.2817	0.9002	**0.3711**	0.8442	0.3208
Arteriovenous malformation	0.0223	0.8620	0.3590	0.8716	**0.3704**	0.8494	0.2857
Seizures, status epilepticus	0.0348	0.8381	**0.4158**	0.8505	0.3704	0.8440	0.3226
Pneumonia due to adenovirus	0.0123	0.8604	0.1250	0.9065	**0.3077**	0.8792	0.1818
Leukemia (acute, without remission)	0.0287	0.8585	0.2783	0.8845	**0.3059**	0.8551	0.2703
Dissem. intravascular coagulopathy	0.0099	0.9556	**0.5000**	0.9532	0.2857	0.9555	0.2500
Septicemia, other	0.0240	0.8586	0.2400	0.8870	**0.2812**	0.7593	0.0000
Bronchiolitis	0.0162	0.9513	0.2667	0.9395	**0.2703**	0.8826	0.1778
Congestive heart failure	0.0133	0.8748	0.1429	0.8756	**0.2703**	0.8326	0.1364
Upper airway obstruc. (UAO), other	0.0378	0.8206	**0.2564**	0.8573	0.2542	0.8350	0.1964
Diabetes mellitus type I, stable	0.0064	0.7105	0.0000	0.9625	0.2500	0.9356	**0.3333**
Cerebral palsy (infantile)	0.0262	0.8230	**0.2609**	0.8359	0.2500	0.6773	0.0980
Coagulopathy	0.0131	0.7501	0.1111	0.8098	**0.2449**	0.8548	0.1667
UAO, ENT surgery, post-status	0.0302	0.9059	**0.4058**	0.8733	0.2400	0.8364	0.1975
Hypertension, systemic	0.0169	0.8740	0.2105	0.8831	0.2388	0.8216	**0.2857**
Acute renal failure, unspecified	0.0191	0.9242	0.2381	0.9510	0.2381	0.9507	**0.3291**
Trauma, vehicular	0.0308	0.8673	0.2105	0.8649	**0.2381**	0.8022	0.1395
Hepatic fail. (acute necrosis of liver)	0.0176	0.8489	0.2222	0.9239	**0.2308**	0.8598	0.1935
Craniosynostosis (anomalies of skull)	0.0064	0.7824	0.0000	0.9267	**0.2286**	0.8443	0.0315
Prematurity ($<$37 weeks gestation)	0.0321	0.7520	0.1548	0.7542	**0.2245**	0.7042	0.1266
Hydrocephalus, other (congenital)	0.0381	0.7118	0.2099	0.7500	**0.2241**	0.7065	0.1961
Pneumothorax	0.0134	0.8220	0.1176	0.7957	0.2188	0.7552	**0.3243**
Congenital muscular dystrophy	0.0121	0.8427	**0.2500**	0.8491	0.2143	0.7460	0.0800
Cardiomyopathy (primary)	0.0191	0.7508	0.1290	0.6057	**0.2143**	0.6372	0.1818
Pulmonary edema	0.0076	0.8839	0.0769	0.8385	**0.2105**	0.8071	0.0870

Table 2: AUC and F1 scores for individual diagnostic codes.

Classifier Performance on Each Diagnostic Code, Sorted by F1

Condition	Base rate	Msmt. AUC	Msmt. F1	Msmt. + indic. AUC	Msmt. + indic. **F1**	Indic. AUC	Indic. F1
(Acute) pancreatitis	0.0106	0.8712	0.0769	0.9512	**0.2000**	0.8182	0.0571
Tumor, disseminated or metastatic	0.0180	0.7178	0.0938	0.7415	**0.1967**	0.6837	0.1062
Hematoma, intracranial	0.0299	0.7724	**0.2278**	0.8249	0.1892	0.7518	0.1474
Neutropenia (agranulocytosis)	0.0108	0.8285	0.0000	0.8114	0.1852	0.8335	**0.2609**
Arrhythmia, other	0.0087	0.8536	0.0000	0.8977	**0.1818**	0.8654	0.0000
Child abuse, suspected	0.0065	0.9544	**0.2222**	0.8642	0.1818	0.8227	0.0870
Encephalopathy, hypoxic/ischemic	0.0116	0.8242	0.1429	0.8571	**0.1818**	0.8009	0.0800
Epidural hematoma	0.0098	0.7389	0.0455	0.8233	**0.1818**	0.7936	0.1000
Tumor, gastrointestinal	0.0100	0.8112	0.1429	0.8636	**0.1778**	0.8732	0.0984
Craniofacial malformation	0.0133	0.8707	**0.2667**	0.8514	0.1778	0.6928	0.2286
Gastroesophageal reflux	0.0182	0.7571	**0.1818**	0.8554	0.1690	0.7739	0.1600
Pneumonia, bacterial (pneumococ.)	0.0186	0.8876	0.1333	0.8806	**0.1600**	0.8616	0.0000
Pneumonia, undetermined	0.0179	0.8323	0.1481	0.8269	**0.1583**	0.7772	0.0947
Cerebral edema	0.0059	0.8275	0.0000	0.9469	**0.1538**	0.9195	0.1500
Pneumonia due to inhalation	0.0078	0.7917	0.1111	0.8602	**0.1538**	0.8268	0.0566
Metabolic or endocrine disorder	0.0095	0.7718	0.0364	0.6929	0.1538	0.6319	**0.2000**
Disorder of kidney and ureter, other	0.0204	0.8486	**0.2857**	0.8650	0.1500	0.8238	0.2500
Urinary tract infection	0.0137	0.7478	0.1154	0.7402	**0.1481**	0.7229	0.0588
Subdural hematoma	0.0147	0.8270	**0.1449**	0.8884	0.1429	0.8190	0.0476
Near drowning	0.0068	0.8296	0.0741	0.7917	**0.1404**	0.6897	0.0397
Cardiac arrest, outside hospital	0.0118	0.8932	0.0976	0.8791	**0.1379**	0.8881	0.0556
Pleural effusion	0.0113	0.8549	0.1081	0.8186	**0.1351**	0.7605	0.1151
Bronchopulmonary dysplasia	0.0252	0.8309	**0.1915**	0.7952	0.1304	0.8503	0.1203
Hyponatremia	0.0056	0.5707	0.0187	0.7398	**0.1176**	0.8775	0.0000
Suspected septicemia, rule out	0.0143	0.7378	0.0923	0.7402	**0.1029**	0.6769	0.0000
Thrombocytopenia	0.0112	0.7381	0.0822	0.7857	**0.1026**	0.8585	0.0800
(Benign) intracranial hypertension	0.0099	0.8494	0.0000	0.9018	0.1020	0.8586	**0.1224**
Pericardial effusion	0.0055	0.8997	0.0870	0.9085	**0.1017**	0.9000	0.0714
Pulmonary contusion	0.0068	0.9029	0.0606	0.8831	**0.0984**	0.8197	0.0225
Surgery, gastrointestinal	0.0104	0.6705	0.0714	0.6666	**0.0976**	0.5545	0.0233
Respiratory Arrest	0.0062	0.8404	0.0000	0.8741	**0.0952**	0.8127	0.0444
Trauma, abdominal	0.0105	0.7426	**0.1667**	0.8623	0.0930	0.6991	0.0426
Atrial septal defect	0.0107	0.7766	0.0727	0.7765	**0.0909**	0.7197	0.0000
Genetic abnormality	0.0557	0.6629	**0.1324**	0.6470	0.0876	0.5705	0.1165
Arrhythmia, ventricular	0.0062	0.8532	0.0303	0.8703	0.0870	0.8182	**0.1250**
Hematologic disorder, other	0.0114	0.6736	0.0800	0.6898	**0.0870**	0.8074	0.0800
Asthma, stable	0.0171	0.7010	**0.0925**	0.6607	0.0870	0.5907	0.0741
Neurofibromatosis	0.0079	0.8022	0.0469	0.7984	**0.0816**	0.7388	0.0160
Tumor, bone	0.0090	0.8830	0.0727	0.8174	**0.0800**	0.7649	0.0417
Shock, hypovolemic	0.0088	0.7703	0.0000	0.8433	**0.0741**	0.8040	0.0000
Gastrointestinal bleed, other	0.0064	0.8325	0.0541	0.7974	0.0741	0.7996	**0.0909**

Classifier Performance on Each Diagnostic Code, Sorted by F1

Condition	Base rate	**Msmt.** AUC	F1	**Msmt. + indic.** AUC	**F1**	**Indic.** AUC	F1
Chromosomal abnormality	0.0173	0.8047	0.1034	0.7197	0.0714	0.6300	**0.1600**
Encephalopathy, other	0.0093	0.8265	0.1250	0.8736	0.0688	0.8335	**0.1250**
Respiratory syncytial virus	0.0130	0.8876	**0.2857**	0.9145	0.0645	0.8716	0.0930
(Hereditary) hemolytic anemia, other	0.0088	0.7582	0.0548	0.8544	**0.0645**	0.9125	0.0513
Obstructive sleep apnea	0.0185	0.7564	0.0613	0.8200	0.0645	0.8087	**0.1111**
Apnea, central	0.0142	0.7871	**0.1600**	0.8134	0.0625	0.8051	0.0000
Neuromuscular, other	0.0132	0.7163	0.0452	0.7069	**0.0619**	0.6484	0.0392
Anemia, acquired	0.0056	0.7378	**0.1017**	0.7596	0.0615	0.8129	0.0519
Meningitis, bacterial	0.0070	0.4431	0.0000	0.7676	**0.0606**	0.5480	0.0000
Trauma, long bone injury	0.0096	0.8757	0.0952	0.9085	0.0597	0.7946	**0.1176**
Bowel (intestinal) obstruction	0.0104	0.7512	**0.0984**	0.6559	0.0597	0.6936	0.0424
Neurologic disorder, other	0.0288	0.7628	**0.1481**	0.6978	0.0588	0.5971	0.0769
Panhypopituitarism	0.0057	0.7763	0.0000	0.7724	**0.0571**	0.6415	0.0000
Thyroid dysfunction	0.0072	0.6310	0.0369	0.6420	**0.0541**	0.6661	0.0000
Coma	0.0056	0.6483	**0.1250**	0.6823	0.0513	0.7155	0.0000
Spinal cord lesion	0.0133	0.7298	**0.0585**	0.7052	0.0488	0.8168	0.0414
Pneumonia, other (mycoplasma)	0.0188	0.8589	**0.1613**	0.8792	0.0476	0.8424	0.1164
Trauma, blunt	0.0065	0.9156	**0.0513**	0.8138	0.0469	0.7426	0.0177
Surgery, thoracic	0.0058	0.7405	0.0000	0.6948	0.0469	0.6087	**0.0909**
Neuroblastoma	0.0059	0.6526	0.0306	0.7268	**0.0360**	0.7775	0.0346
Obesity	0.0098	0.7503	0.0365	0.6814	0.0351	0.6647	**0.0667**
Obstructed ventriculoperitoneal shunt	0.0073	0.6824	0.0267	0.7114	0.0331	0.7516	**0.0667**
Ventricular septal defect	0.0119	0.6641	**0.1081**	0.5680	0.0294	0.5593	0.0444
Croup Syndrome, UAO	0.0069	0.9418	0.2222	0.9834	0.0000	0.9682	**0.2222**
Sickle-cell anemia, unspecified	0.0080	0.6262	0.0000	0.9627	0.0000	0.8661	**0.1250**
Biliary atresia	0.0063	0.9383	**0.2667**	0.9164	0.0000	0.7589	0.0714
Metabolic acidosis (¡7.1)	0.0083	0.9475	**0.1818**	0.9046	0.0000	0.9143	0.1538
Immunologic disorder, other	0.0094	0.9539	**0.1500**	0.8868	0.0000	0.8969	0.1212
Pulmonary hypertension, other	0.0112	0.9259	**0.2500**	0.8826	0.0000	0.8098	0.0000
Trauma, chest	0.0051	0.9261	0.0000	0.8818	0.0000	0.7820	0.0000
Spinal muscular atrophy	0.0052	0.9666	0.0000	0.8658	0.0000	0.8362	0.0000
Trauma, unspecified	0.0065	0.7153	**0.1481**	0.8657	0.0000	0.8224	0.0594
Bone marrow transplant, status post	0.0097	0.8161	**0.5217**	0.8562	0.0000	0.8505	0.1695
Surgery, orthopaedic	0.0180	0.7839	**0.1029**	0.8192	0.0000	0.7331	0.0000
Gastrointestinal bleed, upper	0.0063	0.8388	0.0000	0.8078	0.0000	0.7256	0.0000
Arrhythmia, supraventricular tachy.	0.0055	0.8178	**0.0385**	0.7867	0.0000	0.8199	0.0000
Congenital central alveolar hypovent.	0.0057	0.7067	0.0000	0.7716	0.0000	0.7282	0.0000
Tetralogy of fallot	0.0061	0.5759	0.0000	0.7614	0.0000	0.7637	0.0000
Cardiac disorder, other	0.0071	0.7229	**0.0519**	0.7552	0.0000	0.6287	0.0000
Hydrocephalus, shunt failure	0.0083	0.7715	0.0000	0.7542	0.0000	0.7986	**0.0635**
Cerebral infarction (CVA)	0.0058	0.6766	0.0000	0.7495	0.0000	0.7148	**0.1333**
Congenital heart disorder, other	0.0084	0.7590	0.0000	0.7277	0.0000	0.7803	**0.0583**
Gastrointestinal disorder, other	0.0139	0.6755	0.0336	0.6821	0.0000	0.6465	**0.1026**
Aspiration	0.0072	0.6727	**0.0533**	0.6734	0.0000	0.6792	0.0333
Dehydration	0.0105	0.7356	**0.0690**	0.6636	0.0000	0.5899	0.0000
Tumor, thoracic	0.0077	0.6931	**0.0513**	0.6249	0.0000	0.6815	0.0292
UAO, extubation, status post	0.0085	0.8295	**0.0672**	0.6063	0.0000	0.6128	0.0000

Appendix B. Missing

In this appendix, we present information about the sampling rates and missingness characteristics of our 13 variables. The first column lists the average number of measurements per hour in all episodes with at least one measurement (excluding episodes where the variable is missing entirely). The second column lists the fraction of episodes in which the variable is missing completely (there are zero measurements). The third column lists the missing rate in the resulting discretized sequences.

Variable	**Msmt./hour**	**Missing entirely**	**Frac. missing**
Diabstolic blood pressure	0.5162	0.0135	0.1571
Systolic blood pressure	0.5158	0.0135	0.1569
Peripheral capillary refall rate	1.0419	0.0140	0.5250
End-tidal CO_2	0.9318	0.5710	0.5727
Fraction inspired O_2	1.3004	0.1545	0.7873
Total glasgow coma scale	1.0394	0.0149	0.5250
Glucose	1.4359	0.1323	0.9265
Heart rate	0.2477	0.0133	0.0329
pH	1.4580	0.3053	0.9384
Respiratory rate	0.2523	0.0147	0.0465
Pulse oximetry	0.1937	0.0022	0.0326
Temperature	1.0210	0.0137	0.5235
Urine output	1.1160	0.0353	0.5980

Table 3: Sampling rates and missingness statistics for all 13 features.